## EXCHANGE CURRENTS IN RADIATIVE HYPERON DECAYS

## GEORG WAGNER

 $Centre\ for\ the\ Subatomic\ Structure\ of\ Matter\ (CSSM)\ University\ of\ Adelaide, \\ Australia\ 5005$ 

A short overview of motivations and successes of two-body exchange currents between constituent quarks for electromagnetic hadron observables like charge radii, magnetic and quadrupole moments is given. We then predict and analyze exchange current effects on the radiative decay widths of decuplet hyperons, which are to be measured soon. In our chiral constituent quark model, exchange currents dominate the E2 transition amplitude, while they largely cancel for the M1 transition amplitude. Strangeness suppression of the radiative hyperon decays is weakened by exchange currents. The  $SU_3(F)$  flavor symmetry breaking for the negatively charged hyperons is strong.

#### 1 Introduction

The naive quark model successfully describes baryon magnetic moments. Assuming isospin symmetry  $\mu_u = -2\mu_d$ , without parameters, the proton to neutron magnetic moment ratio -3/2 is close to the experimental value:

$$\mu_p = \frac{4\mu_u - \mu_d}{3} , \ \mu_n = \frac{4\mu_d - \mu_u}{3} \Rightarrow \frac{\mu_p}{\mu_n} = -\frac{3}{2} \simeq \frac{2.793}{-1.913}$$
 (1)

In this impulse approximation – sketched in Figure 1(a) – the photon probing the hadron is absorbed on a single quark, with the two other quarks acting as spectators. If this picture were correct, observables like the neutron charge radius or the quadrupole moment of the nucleon or the  $\Delta$  could only be described by d-state deformations in the hadron wave functions. Deformations arise from residual tensor interactions between quarks. These arguments led to recently performed measurements <sup>1</sup> of the photo-production of the  $\Delta$ -resonance off the nucleon, by which one wishes to extract informations on the deformations of the nucleon and/or  $\Delta$  by the electric quadrupole to magnetic dipole ratio of the transition amplitudes.

In contrast to the above ideas, the baryon mass spectrum gives no evidence of strong tensor forces between quarks. Furthermore, in low-energy QCD the quasi-particle constituent quarks are strongly correlated, interacting for example via the pseudoscalar meson cloud surrounding them. The impulse approximation violates the continuity equation for the electromagnetic current and two-body exchange currents, where the photon momentum is distributed among constituent quarks via their interactions (sketched in Figures 1(b) – 1(e)), have to be consistently introduced.

In recent years, several works  $^{2,3,4,5}$  have studied the effect of two-body exchange currents on electromagnetic baryon observables. A first important observable for exchange currents is the negative square charge radius of the neutron  $^6$   $r_n^2 = -.113(3)$  fm<sup>2</sup>. Within different models  $^{2,7,8}$ , its value has been clearly assigned to the non-valence degrees of freedom in the nucleon. One of these models, namely the concept of exchange currents  $^2$ , allows to derive an analytic relation for  $r_n^2$  and the  $\Delta$ -nucleon mass splitting which is due to the residual spin-dependent interactions between quarks

$$r_n^2 = -\frac{M_\Delta - M_N}{M_N} \, b_N^2 \ . \tag{2}$$

It is fulfilled for a quark core size  $b_N$ =0.61 fm, which is the only model parameter in Eq. (2). The intimate connection of electromagnetic and hadronic observables in Eq. (2) is due to the continuity equation for the electromagnetic current (see below, Eq. (4)) which relates the two-body interactions in the quark model Hamiltonian and the two-body components (exchange currents) in the current operator  $^a$ .

In this contribution we discuss where exchange currents are important and why the magnetic moment results sketched in Eq. (1) remain valid after introduction of exchange currents  $^3$ . We then analyze exchange current effects in the radiative hyperon decays  $^9$ . We demonstrate the possible dominance of exchange currents in the E2/M1 ratios and study their  $SU_3(F)$  symmetry breaking properties.

## 2 Exchange currents in the chiral constituent quark model

## 2.1 Hamiltonian, wave functions, parameters and baryon masses

Constituent quarks emerge as the effective quasi-particle degrees of freedom in hadron physics due to the spontaneously broken chiral symmetry of low-energy QCD. A non-relativistic realisation of the chiral quark model Hamiltonian in the case of three quark flavors u, d, s is  $^{4,9}$ 

$$H = \sum_{i=1}^{3} \left( m_i + \frac{\mathbf{p}_i^2}{2m_i} \right) - \frac{\mathbf{P}^2}{2M} + \sum_{i < j}^{3} \left( V^{\text{Conf}}(i, j) + V^{\text{PS}}(i, j) + V^{\text{OGE}}(i, j) \right)$$
(3)

Here, a quadratic confinement potential  $V^{\mathrm{Conf}}$  is used. The radial form of the confinement potential is according to our experience not crucial for the

<sup>&</sup>lt;sup>a</sup>In impulse approximation in a configuration mixing calculation with d-state admixtures, one needs a much to big quark core size of  $b_N \sim 1$  fm to describe  $r_n^2$ . Using a value of  $b_N \sim 0.6$  fm as required for other hadronic observables, one obtains a much to small neutron charge radius of  $r_n^2 = -.03$  fm².

discussion of hadronic ground state properties. The pseudoscalar meson octet (PS), that constitute the Goldstone bosons of the symmetry breaking, provide the intermediate range interactions between quarks  $V^{\rm PS}$ . We use experimental PS-meson masses and one universal cut-off parameter  $\Lambda=4.2~{\rm fm}^{-1}$  for regularisation. The quark-meson coupling constant is related to the pion-nucleon coupling. The  $\sigma$ -meson as the chiral partner of the pion is included <sup>3</sup> whereas the heavier scalar partners of the Kaon and  $\eta$  are neglected. At short range, the residual interactions comprise one-gluon exchange  $V^{\rm OGE}$  in Fermi-Breit form without retardation corrections <sup>10</sup>.

Table 1: Individual contributions of Hamiltonian (3) to octet and decuplet hyperon masses (quark masses, kinetic energy, confinement potential, one-gluon-, pseudoscalar meson- (PS) and  $\sigma$ -exchange potentials). Experimental values <sup>11</sup> average over particles with different charge. All quantities are given in [MeV].

[MeV]	$\sum_i m_i$	Kin.	Conf.	Gluon	PS	$\sigma$	Total	Exp. <sup>11</sup>
N	939	497	204	-531	-115	-54	939	939
$\Sigma$	1195	497	173	-562	-51	-65	1188	1193
Λ	1195	497	173	-588	-88	-65	1124	1116
Ξ	1451	497	143	-652	-45	-78	1316	1318
Δ	939	497	204	-326	-27	-54	1232	1232
$\Sigma^*$	1195	497	173	-423	-18	-65	1359	1385
$\Xi^*$	1451	497	143	-561	-13	-78	1439	1535
$\Omega$	1707	497	112	-595	-12	-95	1615	1672

We use spherical  $(0s)^3$  oscillator states  $^3$  (containing symmetry breaking effects by the quark masses  $m_s \neq m_d$ ) and  $SU_{SF}(6)$  spin-flavor states for the baryon wave functions. For chosen quark masses  $m_u = m_N/3 = 313$  MeV and  $m_u/m_s = 0.55$ , the effective quark-gluon coupling, the confinement strength and the wave function oscillator parameter  $b_N$  are determined from the baryon masses  $^9$ . Results for the octet and decuplet ground state masses are shown in Table 1.

## 2.2 Continuity equation, electromagnetic currents, and magnetic moments

For illustration, use the Fourier-transformed Heisenberg equation of motion for the charge density  $i\partial/\partial t \,\rho(\vec{x},t) = [H,\rho(\vec{x},t)]$  in the continuity equation for the electromagnetic current  $\partial_{\mu}j^{\mu} = 0$ :

$$\vec{q} \cdot \vec{j}(\vec{q}) = [H, \rho(\vec{q})] \quad . \tag{4}$$

Eq. (4) shows, that for point charges  $\rho(\vec{q}) = e_i \exp(i\vec{q} \cdot \vec{r_i})$  interacting by a Hamiltonian H, momentum- and/or flavor-dependent interactions in H have their corresponding electromagnetic two-body current operators  $\vec{j}$ .

Only the longitudinal part of the three-vector current is determined by Eq. (4). The electromagnetic currents to be included for Hamiltonian (3) are

either constructed by minimal substitution or like in the present case by non-relativistic reduction of the relevant Feynman diagrams <sup>4</sup> shown in Figure 1. The extension of the exchange current operators to three quark flavors can be found in <sup>3,9</sup>. The spatial components for example satisfy the continuity equation (4) with Hamiltonian (3) to order  $\mathcal{O}(1/m_q)$ .

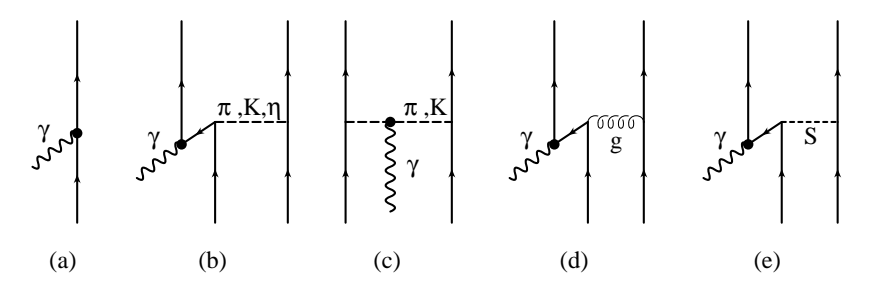


Figure 1: Electromagnetic one- and two-body currents as required by the continuity equation. (a) Impulse approximation, (b) PS-meson pair current  $(\pi, K, \eta)$ , (c) PS-meson in-flight current  $(\pi, K)$ , (d) gluon-pair current, and (e) scalar exchange current (confinement and  $\sigma$ -exchange).

Results for the magnetic moments of the octet baryons  $^3$   $\mu_B \propto \langle B|j^+|B\rangle$  are given in Table 2. Individual exchange current contributions can be as large as 40% of the impulse approximation. We observe substantial cancellations between the gluon-pair- and the scalar-pair-currents (confinement and one-sigma-exchange). Second, partial cancellations between the PS-meson in-flight and the PS-meson pair term occur. The PS-mesons play an important role, because they reduce the strong quark-gluon coupling (adding to the  $\Delta$ -nucleon mass splitting) and thus the gluon exchange current contribution.

Table 2: Octet baryon magnetic moments. The impulse and the exchange current contributions are listed separately: PS-meson-pair and PS-meson-in-flight, gluon-pair, confinement-and  $\sigma$ -pair currents. All quantities are given in nuclear magnetons  $\mu_N = \frac{e}{2M_N}$ . Experimental numbers are from  $^{11}$ .

$[\mu_N]$	Imp.	PS-pair	-in-flight	Gluon	Conf.	$\sigma$	Tot.	$\mathrm{Exp.}^{11}$
p	3.00	-0.13	0.41	0.62	-1.30	0.35	2.94	2.793
n	-2.00	0.19	-0.41	-0.21	0.87	-0.23	-1.79	-1.913
$\Sigma^+$	2.85	-0.00	0.07	0.80	-1.06	0.37	3.02	$2.458 \pm .01$
$\Sigma^0$	0.85	-0.02	0.03	0.17	-0.29	0.10	0.84	
$\Sigma^-$	-1.15	-0.05	0	-0.47	0.48	-0.16	-1.35	$-1.160 \pm .025$
Λ	-0.55	0.03	-0.03	0.03	0.10	-0.05	-0.46	$-0.613 \pm .004$
$\Lambda \leftrightarrow \Sigma^0$	1.73	-0.15	0.26	0.26	-0.67	0.23	1.67	$1.610 \pm .08$
$\Xi^0$	-1.40	0.08	-0.07	-0.10	0.34	-0.17	-1.32	$-1.250 \pm .014$
$\Xi^-$	-0.40	-0.02	0	-0.13	0.004	-0.02	-0.55	$-0.651 \pm .003$

Overall, exchange currents provide less than 10% corrections to the magnetic moments. The cancellations are most pronounced in the S=-1 sector, and we observe a nice improvement for the  $\Xi$ 's, in particular we obtain  $|\mu_{\Xi^-}| > |\mu_{\Lambda}|$  in agreement with experiment. Magnetic moments being very sensitive to the quark core size  $b_N$ , one obtains the strongest cancellations and best agreement with experimental data for a core size  $b_N \sim 0.6$  fm in accordance with Eq. (2).

## 2.3 Interrelations between observables

Within the present approach, the  $\Delta$  charge radius is larger than the proton radius by the amount of the neutron radius <sup>4</sup>, i.e. it is given by the isovector charge radius of the nucleon:  $r_{\Delta}^2 = r_p^2 - r_n^2$ . Even more interesting is the analytic result for the quadrupole moment of the  $\Delta^+$  and the C2 (E2) multipole amplitude in the  $\gamma N \leftrightarrow \Delta$  transition <sup>4</sup>:

$$Q_{\Delta^{+}} = \sqrt{2} \cdot Q_{\gamma N \leftrightarrow \Delta} = r_n^2 = -b_N^2 \frac{m_{\Delta} - m_N}{m_N} \qquad . \tag{5}$$

Quark model calculations using D-state admixtures obtain values three to four times smaller, while the exchange current result of Eq. (5) gives the correct empirical <sup>11</sup> quadrupole transition amplitude  $\left(r_n^2\right)^{\exp} = 1.5 \cdot Q_{\gamma N \leftrightarrow \Delta}^{\exp}$ . Again, using  $(0s)^3$  wave functions, we connect and explain observables by the same non-valence degrees of freedom, the spin-dependent interactions between constituent quarks. At the prize of using simplifying model dynamics, we obtain a qualitative understanding of experimental facts, even including a good agreement with data.

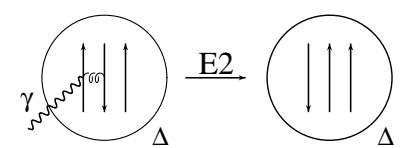


Figure 2: Two-body spin flip induced by gluonic and PS-meson exchange currents.

In Eq. (5), we used Siegert's theorem in the long wavelength limit, which connects C2 and E2 amplitudes and allows to calculate the E2 form factor at small momentum transfers from the charge density  $\rho(\mathbf{q})$ . Technically, only the gluon- and PS-meson-pair charge density operators can contribute for spherical wave functions. Their tensorial structure in spin-space allows for a double spin-flip of the two participating quarks  $\boldsymbol{\sigma}_i^+\boldsymbol{\sigma}_j^-$  as the only mechanism by which an E2 (or C2) photon can be absorbed <sup>4</sup>. This process is sketched in Figure 2 for the case of the  $\Delta$  quadrupole moment (for a  $\Delta$  with  $S_i S_z = 3/2, 1/2$ ).

## 3 Radiative hyperon decays

Current experimental programs aim at a detailed measurement of the radiative decays of some  $\Sigma^*$  and  $\Xi^*$  hyperons <sup>12</sup>. Many model calculations have been performed. Besides the pioneering study of Lipkin and quark model impulse approximation predictions <sup>13</sup> (there, neglecting exchange currents and D-state admixtures, all decays are pure M1 transitions), hyperon decays have been studied for example in  $SU_F(3)$  Skyrme models <sup>14</sup>, chiral bag models <sup>8</sup>, heavy baryon chiral perturbation theory <sup>15</sup>, or in a quenched lattice calculation <sup>16</sup>.

The reasons for increased interest in these observables are twofold. Certainly, as for  $\gamma N \leftrightarrow \Delta$ , the E2/M1 ratios in the radiative hyperon decays contain information on deformations, if not of the valence quarks, then of the non-valence-quark distributions in the baryons. Comparison of model predictions with experiment may provide another signal of exchange currents and may pin down the importance of vector (gluon) vs. pseudoscalar degrees of freedom in the effective quark-quark interaction.

Second, the decays are sensitive to  $SU_F(3)$  flavor symmetry breaking. The decay widths of the negatively charged hyperons  $\Sigma^{*-} \to \gamma \Sigma^-$  and  $\Xi^{*-} \to \gamma \Xi^-$  are zero in a  $SU_F(3)$  flavor-symmetric world. It has been speculated <sup>14</sup> that these decays remain almost forbidden even after  $SU_F(3)$  symmetry breaking. Strangeness suppression, i. e. the decrease of the decay amplitude with increasing strangeness of the hyperon, is best studied comparing transitions involving wave functions which are identical except for the replacement of d- by s-quarks, like  $\gamma N \leftrightarrow \Delta^0$  and  $\gamma \Xi^0 \leftrightarrow \Xi^{*0}$ .

## 3.1 Magnetic dipole transition amplitudes

The various contributions to the M1 and E2 (using Siegert's theorem) transition moments defined in  $^{4,9}$  are given in Tables 3 and 4. Individual exchange current contributions to the M1 moments can be as large as 60% of the impulse approximation. Like for the octet baryon magnetic moments  $^3$  in Table 2, substantial cancellations between gluon-pair- and scalar-pair-currents (confinement and one-sigma-exchange) occur for all decays. Due to partial cancellations between the PS-meson in-flight and the PS-meson pair term, the total PS-meson contribution to the M1-amplitude is again small.

Exchange currents thus provide less than 10% overall corrections to the transition magnetic moments. However, some striking systematics are observed. Strangeness suppression in impulse approximation, i. e. in a picture of valence quarks only, is considerable due to  $m_u/m_s = 0.55-0.6$  (first column in Table 3). Exchange currents decrease the  $\gamma N \leftrightarrow \Delta M1$  moment, slightly decrease the decay amplitudes in the S=-1 sector and slightly increase the

result for the S=-2 sector. Therefore, strangeness suppression is for all six strange decays considerably reduced when exchange currents are included  $^b$ . Strangeness suppression is mostly strong in Skyrme model calculations  $^{14}$ , while lattice results from  $^{16}$  agree reasonably well with our predictions.

Table 3: Transition magnetic moments  $\mu$  of decuplet baryons. The impulse and the various exchange current contributions are listed separately, like in table 2. All quantities are given in nuclear magnetons  $\mu_N = \frac{e}{2M_N}$ . Experimentally known is the non-strange  $\Delta^+ \to \gamma p$  transition magnetic moment  $\mu_{\Delta^+ \to p}^{exp} = 3.58(9)~\mu_N^{-11}$ .

$[\mu_N]$	Imp.	PS-pair	-in-flight	Gluon	Conf.	$\sigma$	Tot.
$\gamma N \leftrightarrow \Delta$	2.828	-0.274	0.586	0.292	-1.228	0.327	2.533
$\gamma \Sigma^+ \leftrightarrow \Sigma^{*+}$	2.404	-0.068	0.097	0.366	-0.822	0.291	2.267
$\gamma \Sigma^0 \leftrightarrow \Sigma^{*0}$	-0.990	0.036	-0.049	-0.095	0.278	-0.105	-0.924
$\gamma \Sigma^- \leftrightarrow \Sigma^{*-}$	-0.424	-0.004	0	-0.176	0.267	-0.082	-0.419
$\gamma\Lambda\leftrightarrow\Sigma^{*0}$	2.449	-0.212	0.366	0.371	-0.944	0.323	2.354
$\gamma \Xi^0 \leftrightarrow \Xi^{*0}$	2.404	-0.117	0.097	0.431	-0.716	0.329	2.428
$\gamma\Xi^-\leftrightarrow\Xi^{*-}$	-0.424	0.009	0	-0.190	0.235	-0.090	-0.460

The transition magnetic moments for the negatively charged hyperons ( $\sim$  0.4 $\mu_N$ ) deviate considerably from the SU<sub>F</sub>(3) flavor-symmetric value 0, when the quark mass ratio  $m_u/m_s$ =0.55 is used.

An interesting comparison can be made for the M1 moments of  $\gamma \Sigma^+ \leftrightarrow \Sigma^{*+}$  and  $\gamma \Xi^0 \leftrightarrow \Xi^{*0}$  or  $\gamma \Sigma^- \leftrightarrow \Sigma^{*-}$  and  $\gamma \Xi^- \leftrightarrow \Xi^{*-}$ . They are pairwise equal in impulse approximation (cf. Table 3), and would also be equal after inclusion of exchange currents if  $SU_F(3)$  flavor symmetry was exact. Gluonand scalar-exchange currents lead to deviations of the order of 10%. Other model calculations differ qualitatively (both in signs and magnitudes) from our prediction for the  $SU_F(3)$  violation of these sum rules.

# 3.2 E2 transition amplitudes, E2/M1 ratios and decay widths

It seems that the M1 transition moments should be measured to very high accuracy if one wishes to discriminate between models or to establish clear signals for exchange currents. Furthermore, most approaches underestimate the only empirically known transition magnetic moment  $\mu_{\Delta^+ \to p}^{\rm exp} = 3.58(9)~\mu_N$  and decay width  $\Gamma_{\Delta \to \gamma N}^{\rm exp} = 610$ –730 keV  $^{11}$ . This problem has not been solved by the exchange currents included here. More promising are the E2 transition

 $<sup>^{</sup>b}$ In particular, the reduction of the  $\gamma\Xi^{0}\leftrightarrow\Xi^{*0}$  impulse result  $\mu_{\mathrm{imp}}^{\gamma\Xi^{0}\leftrightarrow\Xi^{*0}}=2.404\mu_{N}$  as compared with the  $\gamma n\leftrightarrow\Delta^{0}$  transition magnetic moment  $\mu_{\mathrm{imp}}^{\gamma n\leftrightarrow\Delta^{0}}=2.828\mu_{N}$  practically disappears when exchange currents are included, and we obtain  $\mu_{\mathrm{tot}}^{\gamma n\leftrightarrow\Delta^{0}}\simeq\mu_{\mathrm{tot}}^{\gamma\Xi^{0}\leftrightarrow\Xi^{*0}}=2.428\mu_{N}$ .

amplitudes. Our calculated E2 transition amplitude for  $\gamma N \leftrightarrow \Delta$  of –.089 fm² agrees with the recent experimental data  $^{18,19}$   $Q^{\rm exp}_{\Delta^+\to p}=-0.085(13)~{\rm fm^2}.$ 

The hyperon transition quadrupole moments shown in Table 4 receive large contributions from the PS-meson and gluon-pair diagrams of Fig. 1b and Fig. 1d. We recall that the E2 moments would be zero in impulse approximation for spherical valence quark configurations, which we used here. E2 transition moments for negatively charged hyperons  $\Xi^{*-}$  and  $\Sigma^{*-}$  deviate from the  $SU_F(3)$  flavor-symmetric value 0. The gluon contributes strongly to most transition quadrupole moments, on the average  $\sim 2/3$  of the total E2 moment. The experiments may give important hints on the relevance of effective gluon degrees of freedom in hadron properties. Our results are mostly larger in magnitude than Skyrme model results  $^{14}$ , but somewhat smaller than recent lattice results  $^{16}$ .

Table 4: Transition quadrupole moments Q of decuplet baryons. The gluon-pair  $(Q_{\rm g})$  and individual PS-meson  $(\pi,K,\eta)$  exchange current contributions are listed separately. All transition quadrupole moments are given in [fm²]. The last two columns contain the radiative decay widths  $\Gamma$  in [keV] and E2/M1 ratios in [%]. Note that our results are given at  ${\bf q}^2$ =0. Experimentally known is the non-strange decay width  $\Gamma^{exp}_{\Delta\to\gamma N}$ =610–730 keV <sup>11</sup>.

$[fm^2]$	$Q_{ m g}$	$Q_{\pi}$	$Q_K$	$Q_{\eta}$	$Q_{\mathrm{Tot}}$	$\Gamma [\text{keV}]$	E2/M1~[%]
$\gamma N \leftrightarrow \Delta$	058	027	0	004	089	350	-3.65
$\gamma \Sigma^+ \leftrightarrow \Sigma^{*+}$	051	036	.005	009	091	105	-2.9
$\gamma \Sigma^0 \leftrightarrow \Sigma^{*0}$	.016	.009	.002	.002	.030	17.4	-2.3
$\gamma \Sigma^- \leftrightarrow \Sigma^{*-}$	.018	.018	010	.006	.032	3.61	-5.5
$\gamma\Lambda\leftrightarrow\Sigma^{*0}$	041	0	013	.006	047	265	-2.0
$\gamma \Xi^0 \leftrightarrow \Xi^{*0}$	035	0	005	.001	039	172	-1.3
$\gamma \Xi^- \leftrightarrow \Xi^{*-}$	.012	0	.010	006	.016	6.18	-2.8

The decay width  $\Gamma \propto |A_{3/2}|^2 + |A_{1/2}|^2$  is related to the helicity amplitudes  $A_{3/2}$  and  $A_{1/2}$ , which can be expressed as linear combinations of the M1 and E2 transition formfactors  $^{4,17}$ . The E2/M1 ratio of the transition amplitudes is commonly defined as  $E2/M1 = \frac{\omega M_0}{6}Q/\mu$ , where the resonance frequency  $\omega$  is given in the c.m. system of the decaying hyperon. In Table 4, both observables are shown in the last two columns. Due to cancellations of exchange current contributions to the M1 transition amplitude and the relative smallness of the E2 amplitude, the decay widths  $\Gamma$  are dominated by the M1 impulse approximation, i. e. by the simple additive quark model picture with valence quarks only. Only restricted informations on non-valence quark effects should be expected from the experiments here, similar to the situation for the octet magnetic moments.

All model calculations yield large (the largest) E2/M1 ratios for negatively charged states. However, there are important differences. The E2/M1 ratio for

the decays of negatively charged hyperons are particularly model dependent<sup>14</sup> due to the smallness of both the E2 and M1 contributions. Similarly, the  $\gamma \Sigma^0 \leftrightarrow \Sigma^{*0}$  E2/M1 ratio in the Skyrme model approaches is zero <sup>14</sup>, or almost zero, while the  $SU_F(3)$  symmetry breaking and the gluon-pair current in our model allow a sizeable E2/M1 ratio of -2.3%.

# 4 Summary

We have given a brief overview on the concept of exchange currents and predicted and discussed exchange current effects on the radiative decays of decuplet hyperons, which are to be measured soon. In quark potential model descriptions of hadron properties, two-body exchange currents are necessary to satisfy the continuity equation for the electromagnetic current. Exchange currents naturally explain the negative mean square neutron charge radius. Additive magnetic moments results (impulse approximation) remain valid since exchange currents provide only 10% corrections due to cancellations. Observables which are dominated by non-valence d.o.f. like  $r_n^2, Q_\Delta, Q_{\gamma N \leftrightarrow \Delta}$  are well described by exchange currents, and simple analytic relations between observables can be derived. The exchange current concept helps to gain qualitative insight in physical origins of hadron phenomenology.

The widths of the radiative hyperon decays are determined by the impulse approximation M1 transition, due to cancellation effects for the M1 exchange current contributions and the smallness of the E2 transition. In contrast, exchange currents dominate the E2/M1 ratios, where the gluon- and PS-meson-pair charge densities lead to non-zero E2 amplitudes for all hyperon decays. Experimental results on the E2/M1 ratios may provide a good test for the relative importance of effective gluon versus pseudoscalar degrees of freedom in low-energy QCD.

Individual M1 and in particular E2 transition amplitudes are sensitive to  $SU_F(3)$  flavor symmetry breaking and allow to discriminate between models. Violations of impulse approximation or  $SU_F(3)$  flavor symmetry sum-rules are strongly model dependent. In our calculation, strangeness suppression is weakened by exchange currents. The decay widths of the negatively charged hyperons deviate considerably from the  $SU_F(3)$  flavor symmetric value.

## Acknowledgments

The work reported here has been performed in collaboration with A. J. Buchmann and Amand Faessler (University of Tübingen, Germany). I thank the Deutsche Forschungsgemeinschaft (DFG) for a postdoctoral fellowship (contract number WA1147/1-1).

#### References

- 1. see Prog. Part. Nucl. Phys. 34, 43 (1995) and references therein.
- A. J. Buchmann, E. Hernández, and K. Yazaki, *Phys. Lett.* B269, 35 (1991); *Nucl. Phys.* A569, 661 (1994).
- G. Wagner, A. J. Buchmann, and A. Faessler, Phys. Lett. B359, 288 (1995).
- A. J. Buchmann, E. Hernández, and A. Faessler, Phys. Rev. C55, 448 (1997).
- U. Meyer, A. J. Buchmann, and A. Faessler, *Phys. Lett.* B408, 19 (1997).
- S. Kopecky, P. Riehs, J. A. Harvey, and N. W. Hill, *Phys. Rev. Lett.* 74, 2427 (1995).
- 7. C. V. Christov et al., Prog. Part. Nucl. Phys. 37, 91 (1996).
- D. H. Lu, A. W. Thomas, A. G. Williams, Phys. Rev. C57, (1998), Phys. Rev. C55, 3108 (1997).
- 9. G. Wagner, A. J. Buchmann, and A. Faessler, submitted to *Phys. Rev.* C, (1998).
- 10. A. DeRujula, H. Georgi, and S.L. Glashow, *Phys. Rev.* **D12**, 147 (1975).
- 11. Particle Data Group, R. M. Barnett et al., Phys. Rev. D54, 1 (1996).
- J. S. Russ, Nucl. Phys. A585, 39c (1995); R. A. Schumacher, Nucl. Phys. A585, 63c (1995).
- H. J. Lipkin, *Phys. Rev.* **D7**, 846 (1973); J. W. Darewych, M. Horbatsch, and R. Koniuk, *Phys. Rev.* **D28**, 1125 (1983); E. Kaxiras, E. J. Moniz, and M. Soyeur, *Phys. Rev.* **D32**, 695 (1985).
- T. Haberichter, H. Reinhardt, N. N. Scoccola, H. Weigel, Nucl. Phys. A615, 291 (1997); A. Abada, H. Weigel, H. Reinhardt, Phys. Lett. B366, 26 (1996); Y. Oh, Mod. Phys. Lett. A10, 1027 (1995); C. L. Schat, C. Gobbi, N. N. Scoccola, Phys. Lett. B356, 1 (1995).
- M. N. Butler, M. J. Savage, and R. P. Springer, *Phys. Lett.* B304, 353 (1993).
- D. B. Leinweber, T. Draper, R. M. Woloshyn, *Phys. Rev.* **D48**, 2230 (1993).
- 17. M. M. Giannini, Rep. Prog. Phys. **54**, 453 (1990).
- 18. R. Beck, et al., Phys. Rev. Lett. 78, 606 (1997).
- O. Hanstein, D. Drechsel and L. Tiator, *Phys. Lett.* B385, 45 (1996); see also: nucl-th/9709067.